Solvent Effect on the Conformational Equilibrium of 1,2-Dichloroethane in Water. The Role of Solute Polarization

Sergio Madurga and Eudald Vilaseca*

Departament de Química Física i Centre Especial de Recerca en Química Teòrica, Facultat de Química, Universitat de Barcelona, Martí i Franquès 1, 08028-Barcelona, Catalunya, Spain

Received: February 26, 2004; In Final Form: June 17, 2004

The conformational equilibrium of the 1,2-dichloroethane molecule in water has been studied with Monte Carlo free energy perturbation simulations. A polarizable model for the solute molecule combined with the nonpolarizable TIP4P model for the water molecules has been employed. The approach of only taking into account the polarization of solute produces a rather small increase of computational time with respect to the nonpolarizable simulations. Relative solvation free energies of the trans and gauche 1,2-dichloroethane conformations have been calculated through three perturbation paths which correspond to the progressive incorporation of three different intermolecular solute−solvent energy contributions (van der Waals, Coulombic, and polarization). This stepped procedure allows the separate analysis of the different interaction forces. The solute polarization is studied by introducing atom polarizabilities in the 1,2-dichloroethane molecule. Three polarization procedures which differ in the treatment of the intramolecular interactions among the polarization sites of the solute molecule have been analyzed. It is found that the inclusion of solute polarization produces a different reorganization of solvent molecules around the 1,2-dichloroethane conformations.

1. Introduction

1,2-dichloroethane (DCE) is a prototype flexible polar molecule which shows a great dipole moment variation between its conformational minima. It is well-known that the position of its trans−gauche conformational equilibrium is related with the polarity of the solvent, the polar gauche conformer being favored in solvents with higher dielectric constants.[1−6] Molecular dynamics calculations of DCE in water have shown a marked shift of the solute with respect to gas phase toward the gauche conformation as a result of, mainly, the Coulombic solute−solvent interactions.[7−9] Similar results are obtained in Monte Carlo (MC) or molecular dynamics simulations performed for DCE in methyl chloride,[6] in acetonitrile,[10] or in pure liquid.[11−14] On the other hand, the solvent effect observed in nonpolar solvents produces also an increase of the gauche population. In these cases, the gauche shift, reproduced with MC simulations in carbon tetrachloride[15] and in cyclohexane,[4] is attributed to the polarization interactions. There is also a recent study of the aqueous DCE solution employing a continuum solvation method coupled with a MC conformational search[16] that shows a large influence of solvation on the relative population between minima and on the general shape of the conformational free energy surface. However, the explicit consideration of the polarization interactions has not been previously described in discrete simulations of this conformational equilibrium in water.

Explicit polarizable force fields have been used in a variety of systems with improved results with respect to the pairwise additive force fields. In particular, the consideration of nonadditive effects has proved to be necessary in the description of cation−π interactions,[17−19] amine solvation,[20] liquid−liquid interfaces,[21,22] aqueous ionic solutions,[23,24] conformational equilibria in solution,[15,25] and liquid properties of water,[26−28] methanol, and *N*-methyl acetamide.[29] Using a perturbation approach, Cubero et al. studied the nature of the cation−π interactions of the benzene series showing that the total electrostatic energy is dominated by the polarization contribution.[30] However, although polarization effects are always present with a higher or lower intensity in the intermolecular interactions, it is known that simple electrostatic models still possess remarkable success in the modeling of molecular systems. The reason is that, in general, there is a good linear relationship between the individual energy terms (van der Waals, Coulombic, and polarization contributions) and the total interaction energy.[31] Thus, in these cases, a simple force field without explicit polarization can adequately model the intermolecular interactions because the polarization effects can be integrated in an average way. However, this simplification may not be valid in a molecule with highly polarizable atoms such as DCE. Thus, in the present work, we consider the explicit solute polarization to analyze the importance of polarization forces in the energetic and structural properties of DCE in water.

The explicit incorporation of electronic polarization effects into molecular-modeling calculations has been the subject of intensive effort over the past years.[32−42] Two main polarization models can be distinguished. The fluctuating-charge model, where the atomic charges fluctuate in response to the environment, and the inducible point-dipole model, where a point dipole is induced at each polarization site in response to the electric fields. In the first model, the fluctuating charges are assigned fictitious masses and are treated as additional degrees of freedom in the equation of motion. On the other hand, in the inducible point-dipole model, several variants can be distinguished depending on the scheme for partitioning the molecular polarizability. One of the most employed is the scheme proposed by Applequist.[43] This is an empirical model that defines atomic dipolar polarizabilities in which the mutual polarization of the atoms is taken into account. Other approaches consist of deriving

* To whom correspondence should be addressed. Fax: 34-93 4021231. E-mail: eudald@qf.ub.es.

10.1021/jp0491358 CCC: $27.50
Published on Web 09/03/2004

atomic polarizabilities from quantum chemical calculations.[44−49] Although better values of molecular polarizabilities can be achieved by these procedures, sophisticated quantum mechanical calculations employing large and flexible basis sets are required, limiting its applicability to molecules of medium and small size. On the other hand, the Applequist model seems to be a promising procedure to obtain good estimations of the intermolecular interaction energy using transferable polarizability values. However, the future application to macromolecular systems requires a better parametrization in conjunction with a reduction of the computational cost. In this work, several polarization procedures have been analyzed, including one scheme that needs no iterative process to obtain the polarization energy. Additionally, an excessive increase of the computational time is avoided by modeling the solution with nonpolarizable solvent molecules and one polarizable solute. The calculation of the conformational equilibrium of DCE in water has been done with free energy perturbation (FEP) simulations and an energy decomposition that allows the relative contributions of various energy terms (van der Waals, Coulombic, and polarization) to the total intermolecular interaction energy to be known. The findings of this work provide additional insights on modeling polarization interactions in molecular mechanics simulations, and the quantitative results will be useful for the development of more efficient force fields based on the Applequist model.

2. Computational Details

The conformational equilibrium of DCE in water has been studied performing FEP calculations with a MC simulation program of our group. The simulated system consisted of one molecule of DCE in a rigid conformation and 1400 molecules of water in a periodic cube of edge ∼35 Å. Simulations were carried out in the isothermal−isobaric (NPT) ensemble at 25 °C and 1 atm using the Metropolis sampling procedure. The Markov chain was generated by selecting a molecule at random and changing, also randomly, its coordinates. The ranges for translational and rotational motion of the solute and solvent molecules and the range of the attempted volume changes were adjusted to yield an approximate acceptance rate of 40%. The internal coordinates of water and DCE molecules were not sampled. Solute motion was performed with a probability of 1.5%, and solvent molecules were selected using the preferential sampling algorithm. This algorithm improves the convergence of solute properties by increasing the sampling of the solvent molecules near the solute. The probability of attempted movements of water molecules was calculated using a weighting function that depends on the solute−solvent distance. The chosen definition is similar to that of previous works:[25,50]

$$w(r_{\min}) = 1/(r_{\min}^{2} + \text{cte}) \tag{1}$$

where cte is a constant with 120 Å^2 value and $r_{\min}$ is defined as the distance between the oxygen atom of a water molecule and its nearest carbon or chloride atom of the DCE molecule. With this definition, the sampling of the solvent molecules near the chloride atoms of the solute is improved. To obtain a correct implementation of this sampling procedure, the acceptance probability in the Metropolis test was modified as usual.[51−53]

Solvation free energy variations between different states of the solute molecule were computed by the FEP method using the usual Zwanzing's perturbation expression

$$\Delta G_{0\rightarrow 1} = -k_B T \ln\langle \exp(-\Delta H/k_B T)\rangle_0 \tag{2}$$

TABLE 1: LJ Parameters, Partial Charges, and Polarizability Values of Atom Sites of DCE Used in the MC Simulations[a]

center	σ (Å)	ϵ (kcal/mol)	q_{trans} (e$^-$)	q_{gauche} (e$^-$)	α (Å^3)
C_1	3.50	0.066	−0.041	−0.108	0.878
C_2	3.50	0.066	−0.041	−0.108	0.878
Cl_3	3.40	0.300	−0.196	−0.161	1.910
Cl_4	3.40	0.300	−0.196	−0.161	1.910
H_5	2.50	0.030	0.118	0.125	0.135
H_6	2.50	0.030	0.118	0.144	0.135
H_7	2.50	0.030	0.118	0.125	0.135
H_8	2.50	0.030	0.118	0.144	0.135

[a] A different set of charge values is given for each conformation. H_5, H_6, and Cl_3 are attached to C_1, and H_7, H_8, and Cl_4 are attached to C_2.

The average refers to sampling configurations for the reference state 0 in the isothermal−isobaric ensemble, k_B is the Boltzmann constant, T is the temperature, and ΔH is calculated as the difference between the total potential energies of states 0 and 1. When these two states differ in more than a trivial way, convergence of eq 2 is reduced. In that case, it is convenient to define a coupling parameter λ so that in going from $\lambda = 0$ to $\lambda = 1$ the system is gradually transformed from the initial to the final state. In our implementation, the geometry parameters (bond lengths, bond angles, and dihedral angles) and the potential function parameters (polarizability and charge values) depend linearly on this coupling parameter. Then, the smooth transformation of any geometrical or potential parameter (ζ) can be expressed as

$$\zeta(\lambda) = \zeta_0 + \lambda(\zeta_1 - \zeta_0) \tag{3}$$

where λ goes from 0 to 1 through a certain number of steps (windows). The Lennard-Jones (LJ) parameters of DCE solute were not transformed and were kept fixed at their standard values (Table 1). The total free energy variation is calculated as the sum of the individual free energy changes of all windows. Each individual free energy is obtained as the average of the forward and backward change values.

Solute geometries of the two conformational minima of the DCE molecule were obtained from optimizations at the MP2/6-31G** level with the GAMESS package.[54]

The relative solvation free energy between trans and gauche DCE conformations has been calculated through a decomposition in several steps (Figure 1). In a first step, the relative free energy of solvation with a simple modeling of the solute is computed ($\Delta G^{SOLV(LJ)}$). The transformation between trans and gauche conformations is performed with FEP simulations using only LJ sites in the DCE molecule. Thus, at this stage, the DCE is treated as a hydrophobic molecule. The second step corresponds to the inclusion of the electrostatic contribution to each individual conformation (ΔG^{Q}). This contribution has been calculated through FEP simulations of a discharge process where the charges of the solute sites are progressively annihilated. Thus, the electrostatic contribution to the free energy is given by the value of the obtained free energy variation with a reversed sign. In the last step, the contribution of the polarization to the free energy of solvation has been computed by introducing the polarization sites through FEP simulations (ΔG^{POL}). As the free energies of these three processes are well separated, the contributions of the LJ, electrostatic, and polarization free energies to the global equilibrium can be analyzed.

As a result, three types of perturbation paths were defined to calculate the free energies of the previous processes: (1) LJ transformations between conformations. Trans and gauche DCE

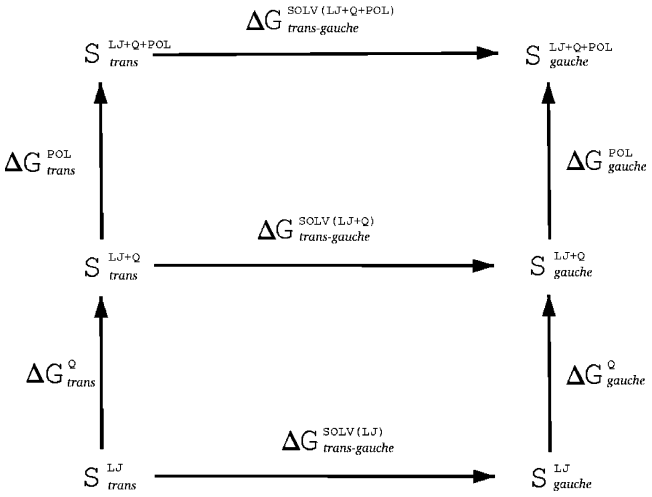

Figure 1. Scheme of the decomposition of the relative solvation energy between the trans (S_{trans}) and gauche (S_{gauche}) conformations of DCE in water.

conformations have been connected through 18 windows. A total of 2×10^6 configurations of equilibration between windows and 10×10^6 configurations of averaging in each window were done. (2) Discharge process. The electrostatic contribution for each conformation was calculated by linearly decreasing the formal charges of solute atoms to 0 through 16 windows. Each window consisted of 1×10^6 configurations of equilibration and 2×10^6 configurations of averaging. (3) Polarization process. The contribution of the polarization energy of each conformation was calculated by linearly introducing the atomic polarizability of each solute atom through 10 windows. Each window consisted of 5×10^5 configurations of equilibration and 3×10^6 configurations of averaging.

The intermolecular interaction energy of the system for the most complete case is calculated as

$$U = U^{\mathrm{PAIR}} + U^{\mathrm{POL}} \tag{4}$$

The U^{PAIR} pairwise additive energetic term includes the LJ and the Coulombic contributions

$$U^{\mathrm{PAIR}} = U^{\mathrm{LJ}} + U^{\mathrm{qq}} \tag{5}$$

The LJ interaction energy of the whole system is given by the sum of all pairs of solvent−solvent and solute−solvent LJ interactions.

$$U^{\mathrm{LJ}} = \sum_{i,j>i}^{N} \sum_{A,B\neq A}^{N_{\mathrm{SLJ}}} 4\epsilon_{A,B}\left[\left(\frac{\sigma_{A,B}}{r_{iA,jB}}\right)^{12} - \left(\frac{\sigma_{A,B}}{r_{iA,jB}}\right)^{6}\right] + U_{\mathrm{LJ}}^{\mathrm{corr}} \tag{6}$$

where N is the total number of molecules of the system and N_{SLJ} is the number of LJ sites in the solute or in the solvent molecules ($N_{\mathrm{SLJ}} = 8$ for DCE and $N_{\mathrm{SLJ}} = 1$ for water). The $r_{iA,jB}$ is the distance of site A in molecule i from site B in molecule j. OPLS all-atom values have been assigned to the LJ parameters for the DCE molecule (Table 1) and the nonpolarizable TIP4P water model[55] was employed for solvent molecules. The usual combining rules were used to calculate ϵ and σ values for DCE−water interactions. The long-range correction for the LJ interactions, $U_{\mathrm{LJ}}^{\mathrm{corr}}$, is calculated assuming that the partial pair-correlation functions between the oxygen atom of water molecules and between the LJ sites of the solute (X_i) and the oxygen of solvent molecules are the unity beyond the cutoff values R_c^{O-O} and $R_c^{O-X_i}$, respectively. Thus,

$$U_{\mathrm{LJ}}^{\mathrm{corr}} = \frac{8\pi\rho_m}{3}\left[N_{H_2O}\frac{\epsilon_{O-O}\sigma_{O-O}^{6}}{(R_c^{O-O})^3}\left[\frac{1}{3}\left(\frac{\sigma_{O-O}}{R_c^{O-O}}\right)^6 - 1\right] + \sum_i N_{\mathrm{SLJ}}^{\mathrm{SOLUTE}}\frac{\epsilon_{O-X_i}\sigma_{O-X_i}^{6}}{(R_c^{O-X_i})^3}\left[\frac{1}{3}\left(\frac{\sigma_{O-X_i}}{R_c^{O-X_i}}\right)^6 - 1\right]\right] \tag{7}$$

where ϵ_{O-O}, σ_{O-O}, ϵ_{O-X_i}, and σ_{O-X_i} are the interaction LJ parameters between water molecules and between water and LJ sites of the solute, respectively. N_{H_2O} is the number of water molecules of the system, ρ_m is the number density of molecules, and $N_{\mathrm{SLJ}}^{\mathrm{SOLUTE}}$ the number of solute LJ sites.

The U^{qq} term in eq 5 is the energy of the system due to charge−charge interactions corrected with the reaction field method:

$$U^{\mathrm{qq}} = \frac{1}{4\pi\epsilon_0}\left[\frac{c_{\mathrm{RF}}}{2}N_{H_2O}\vec{m}_i^{\,2} + \sum_{i,j>i}^{N}\sum_{A,B\neq A}^{N_{\mathrm{Sq}}}\frac{q_A q_B}{r_{iA,jB}}\left(1 + \frac{c_{\mathrm{RF}}}{2}r_{iA,jB}^{\,3}\right)\right] \tag{8}$$

where N_{Sq} is the number of electrostatic sites in the solute or in the solvent molecules. In the DCE molecule the charges are centered on the atoms ($N_{\mathrm{Sq}} = 8$), whereas in the water molecules the TIP4P model was used ($N_{\mathrm{Sq}} = 3$). Charges of the atom sites of each of the DCE conformational minima, q, are fitted to the molecular electrostatic potentials with the CHELPG method implemented in the GAMESS package from its corresponding MP2/6-31G** gas-phase wave function (Table 1). The c_{RF} term is the reaction field correction factor, ϵ_0 is the vacuum permittivity, and $\vec{m}_i$ is the permanent dipole moment of water molecules.

The U^{POL} energy term of eq 4 is the energy contribution due to the polarization of solute sites. This term can be expressed as

$$U^{\mathrm{POL}} = -\frac{1}{2}\sum_{A}^{N_{\mathrm{P}}}\vec{\mu}_A^{\mathrm{ind}}\vec{E}_A^{\mathrm{q}} \tag{9}$$

where N_{P} is the number of polarization sites in the solute molecule ($N_{\mathrm{P}} = 8$). The $\vec{\mu}_A^{\mathrm{ind}}$ induced dipole moment can be given as

$$\vec{\mu}_A^{\mathrm{ind}} = \alpha_A(\vec{E}_A^{\mathrm{q}} + \vec{E}_A^{\mathrm{d}}) \tag{10}$$

where α_A is the polarizability of site A in the solute molecule and $\vec{E}_A^{\mathrm{q}}$ and $\vec{E}_A^{\mathrm{d}}$ are the local electric fields at the position of $\vec{\mu}_A^{\mathrm{ind}}$ produced by the fixed charges of the electrostatic sites and the induced dipole moments of the other polarization sites, respectively. Point polarizabilities were introduced in all atoms of the DCE molecule to account for the nonadditive induced polarization effect. The atomic site polarizabilities were taken from the interaction model of Applequist et al.[56] (Table 1).

The electric fields produced by the permanent charges and by the induced dipole moments can be calculated as

$$\vec{E}_A^{\mathrm{q}} = \frac{1}{4\pi\epsilon_0}\left[\sum_{j}^{N_{H_2O}}\sum_{C}^{N_{\mathrm{Sq}}}\frac{q_C}{r_{A,jC}^{\,3}}\vec{r}_{A,jC}(1 - c_{\mathrm{RF}}r_{A,jC}^{\,3})\right] \tag{11}$$

and

$$\vec{E}_A^{\,d} = \frac{1}{4\pi\epsilon_0}\left[c_{RF}\vec{\mu}_A^{ind} + \sum_{B\neq A}^{N_P}\frac{1}{r_{A,B}^{\,3}}\left[\frac{3\vec{r}_{A,B}\vec{\mu}_B^{ind}}{r_{A,B}^{\,2}}\vec{r}_{A,B} - \vec{\mu}_B^{ind}(1 - c_{RF}r_{A,B}^{\,3})\right]\right] \quad (12)$$

$r_{A,jC}$ being the vector pointing from the position of the charge site C of the solvent molecule j to the site A of the solute and $r_{A,B}$ being the vector pointing from the polarization site B to the polarization site A of the solute. The j sum in eq 11 runs only for the solvent molecules because solute intramolecular interactions among permanent charges are not considered in the present study.

The reaction field correction factor, c_{RF}, can be written as

$$c_{RF} = \frac{2(\epsilon_{RF} - 1)}{2\epsilon_{RF} + 1}\frac{1}{R_c^{\,3}} \quad (13)$$

where ϵ_{RF} is the dielectric constant of the continuum beyond the interaction cutoff distance (R_c). In the solvent−solvent interactions, the R_c cutoff distance was based on the oxygen−oxygen distances (R_c^{O-O}). For LJ and electrostatic terms, the cutoff is set at 8.5 Å while for the polarization terms the cutoff is reduced to 7.0 Å. Solute−solvent interactions are set to 0 when the distance between the water oxygen and its nearest DCE carbon or chloride atom is greater than 12.5 Å for LJ and electrostatic terms and 11.0 Å for polarization terms. The reduction in the polarization cutoff is needed to accelerate the calculation of the polarization energy of the system. This reduction can be done because of the faster decay of the polarization interactions. The polarization energy of the system at every configuration was calculated using eqs 10−12 in an iterative procedure, because the induced dipole moment of each polarization site depends on the induced dipole moments of the other polarization sites. The iterative process was stopped when the variation of the polarization energy between two consecutive cycles was smaller than 0.01 kcal/mol. A more precise criterion, 0.001 kcal/mol, was applied to the system configurations selected for the calculation of the average free energy differences. Statistical uncertainties in the averages were estimated by block averaging.[53]

3. Results and Discussion

3.1. LJ Transformation between Conformations. In the first type of perturbation paths, the solute−solvent interactions were calculated using only LJ parameters and the solute was considered nonpolarizable and uncharged. On the other hand, water−water interactions were described using the LJ site centered in the oxygen in conjunction with the three charge sites of the TIP4P water model. This type of simulations consisted of progressively transforming the trans conformation into the gauche conformation of DCE through 18 windows. A linear variation of bond distances, angles, and torsions of the structure of the solute was carried out to construct the path of transformation. Free energies were calculated using the Zwanzing's expression (eq 2) for the perturbations to the forward and backward structures. In each window, the perturbed solute structure was located in a position that minimized the root-mean-square displacement of all atoms with respect to the unperturbed structure.

The obtained free energy variation value for the conversion between the trans and gauche conformational structures of DCE in water ($\Delta G^{SOLV(LJ)}$) is −0.05 kcal/mol (Table 2). This result is the average of five different free energy LJ transformations, whose values fall in the small range, −0.15 to +0.05 kcal/mol. The mean hysteresis value is 0.06 kcal/mol, and the obtained standard deviation (stdev) for the mean values is 0.04 kcal/mol. Because the free energy for the conversion is similar to the calculated stdev, it is not possible to conclude that the gauche conformation is significantly more solvent stabilized than the trans conformation at the LJ level.

TABLE 2: Free Energy Values Obtained from the FEP Simulations of DCE in Water for the LJ, Electrostatic, and Polarization Contributions[a]

	n	trans	gauche	Δ
ΔG_{Exp}^{GAS}				1.27[b]
$\Delta G^{SOLV(LJ)}$	5			−0.05
ΔG^{Q}	5	−1.89	−2.90	−1.01
$\Delta G^{POL}(q_w, \mu)$	1	−1.92	−2.41	−0.49
$\Delta G^{POL}(q_w, \mu_{1,4})$	1	−0.93	−1.49	−0.56
$\Delta G^{POL}(q_w)$	4	−1.04	−1.56	−0.52

[a] The gauche−trans differences are given in the last column. The experimental gas-phase conformational free energy difference is also displayed. n indicates the number of simulations performed to obtain the free energy values of the trans and gauche conformers. Energies are in kcal/mol. [b] Reference 57.

TABLE 3: Total Free Energy Difference for the Conformational Equilibrium of DCE in Water for Each Solvation Model Considered[a]

	total	% trans	% gauche
ΔG_{Exp}^{GAS}	1.27[b]	81	19
$\Delta G_{Exp}^{GAS} + \Delta G^{SOLV(LJ)}$	1.22	80	20
$\Delta G_{Exp}^{GAS} + \Delta G^{SOLV(LJ)} + \Delta\Delta G^{Q}$	0.21	42	58
$\Delta G_{Exp}^{GAS} + \Delta G^{SOLV(LJ)} + \Delta\Delta G^{Q} + \Delta\Delta G^{POL(q_w,\mu)}$	−0.28	24	76
$\Delta G_{Exp}^{GAS} + \Delta G^{SOLV(LJ)} + \Delta\Delta G^{Q} + \Delta\Delta G^{POL(q_w,\mu_{1,4})}$	−0.35	22	78
$\Delta G_{Exp}^{GAS} + \Delta G^{SOLV(LJ)} + \Delta\Delta G^{Q} + \Delta\Delta G^{POL(q_w)}$	−0.31	23	77
$\Delta G_{Exp}^{SOLUTION}$	−0.02[b]	33	67

[a] ΔG_{Exp}^{GAS} and $\Delta G_{Exp}^{SOLUTION}$ are the gas-phase and solution experimental values. Conformational proportions are indicated for trans and gauche conformations. Energies are in kcal/mol. [b] Reference 57.

The gas-phase free energy difference (ΔG_{Exp}^{GAS}) is 1.27 kcal/mol according to the experimental results reported by Wiberg et al.[1] using the absorption coefficients of DCE in vacuo calculated by Cappelli et al.[57] (Table 2). This free energy difference corresponds to an 81% of trans proportion at 298 K. As can be seen, the absolute value of $\Delta G^{SOLV(LJ)}$ is markedly smaller than the conformational free energy difference in the gas phase. Thus, at this LJ level, the conformational equilibrium of DCE in water is similar to the conformational equilibrium in the gas phase. The calculated proportion for the trans conformation at 298 K is 80%.

The experimental free energy for the conformational equilibrium of DCE in water ($\Delta G_{Exp}^{SOLUTION}$) is −0.02 kcal/mol (Table 3). This free energy was obtained by Cappelli et al.[57] correcting the experimental free energy reported by Kato et al.[58] with the Raman scattering cross sections of the two conformational minima of DCE in water calculated by himself. The experimental proportion of the trans conformation corresponds to 33%, indicating a large influence of solvation on the relative population between minima. Thus, the change in the population of the gauche and trans conformers induced by solvation cannot be reproduced when the solute is modeled with only LJ interactions.

3.2. Discharge Process. Free energy discharge calculations were performed for trans and gauche conformations of DCE through 16 windows. The obtained results (Table 2) show that the free energy variation for the charging process (ΔG^{Q}) is favorable for both, polar (gauche) and nonpolar (trans), conformations of the DCE molecule, the electrostatic stabilization being greater for the gauche conformation. The free energy values for both conformations are the average of five simulations, showing for each mean value a stdev of 0.06 kcal/mol. Adding the first three lines of the last column of Table 2—relative gas-phase free energy, relative conformational LJ free energies, and relative electrostatic free energies—the relative global free energy 0.21 kcal/mol is obtained for the DCE conformations. For this potential model, the global free energy difference is now reduced (Table 3) and the conformational equilibrium is moved to the gauche conformation (58%). Thus, the inclusion of the electrostatic contribution favors the stabilization of the gauche conformation obtaining conformational populations near the experimental value of 67% for the gauche conformation.

As can be seen in Table 1, the assigned CHELPG charge value for the Cl atoms of DCE is for the trans conformation ($-0.196e^{-}$) greater than for the gauche conformation ($-0.161e^{-}$). This bigger charge separation makes the dipole moment of the $Cl-CH_2$ moiety of the trans conformation (2.13 D) to be greater than the corresponding dipole of the gauche conformation (1.92 D). However, the consideration of the two $Cl-CH_2$ moieties produces molecular dipole moments of 0 and 3.11 D for trans and gauche conformations, respectively. Thus, the greater electrostatic stabilization of the gauche conformation can be attributed to this difference in the net dipole moment.

3.3. Polarization Process. To introduce the polarization sites in the atoms of the trans and gauche conformations of the DCE solute solved in a nonpolarizable water, two series of FEP simulations (one for each conformation) have been performed. In addition, three polarization models [POL(q_w), POL(q_w, μ) and POL(q_w, $\mu_{1,4}$)] have been studied. They differ in the way the intramolecular interactions among the polarization sites of DCE are treated.

In the POL(q_w) model, all intramolecular interactions among the induced dipole moments of the solute are neglected. Only the electric field due to the charges of solvent molecules are considered. Thus, the electric fields produced by the induced dipole moments are removed from eqs 10 and 9, giving respectively

$$\vec{\mu}_A^{\,\mathrm{ind}} \approx \alpha_A \vec{E}_A^{\,\mathrm{q}} \tag{14}$$

and

$$U^{\mathrm{POL}} = -\frac{1}{2}\sum_{A}^{N_P} \vec{\mu}_A^{\,\mathrm{ind}} \vec{E}_A^{\,\mathrm{q}} \approx -\frac{1}{2}\sum_{A}^{N_P} \alpha_A \vec{E}_A^{\,\mathrm{q}} \vec{E}_A^{\,\mathrm{q}} \tag{15}$$

The $\vec{E}Q_A$ electric field on a polarization site A of DCE is calculated as a function of only the charges of the TIP4P waters. Thus, charges on the DCE sites do not affect directly the polarization energy terms.

In the POL(q_w, μ) polarization model, all intramolecular interactions among the induced dipole moments of the solute are considered and the electric field they produce ($\vec{E}_A^{\,\mathrm{d}}$) is calculated as indicated in eq 12. On the other hand, in the POL(q_w, $\mu_{1,4}$) model, only the intramolecular 1−4 bonded interactions between the induced dipole moments of the solute are considered in the calculation of $\vec{E}_A^{\,\mathrm{d}}$. All the simulations were performed with the nonpolarizable TIP4P water model. Thus, in the three models, the polarization only takes place in the solute. The calculation of the polarization energy in the POL(q_w, μ) and POL(q_w, $\mu_{1,4}$) models requires an iterative procedure, whereas in the simplest polarization model, POL(q_w), the polarization energy is directly obtained.

All free energy results are shown in Table 2. For the POL(q_w, μ) model, it can be seen that the gauche conformation, the most stabilized by the electrostatic forces, is also the most stabilized by the polarization interactions. Adding all free energy contributions [$\Delta G_{\mathrm{Exp}}^{\mathrm{GAS}}$, $\Delta G^{\mathrm{SOLV(LJ)}}$, ΔG^{Q} and $\Delta G^{\mathrm{POL}}(q_w, \mu)$], the total free energy difference between the trans and the gauche conformations is obtained for this model. The gauche conformation in now about 0.28 kcal/mol more stable than the trans conformation, and from that, the calculated relative proportions are 24 and 76% for trans and gauche, respectively (Table 3). Thus, the gauche conformation is more stabilized than in the LJ + Q model, increasing its conformational proportion to an extent that it exceeds the experimental value. However, both of the conformational results, from the polarizable and nonpolarizable models, are relatively near the experimental proportions of DCE in water.

In the POL(q_w, $\mu_{1,4}$) model, a free energy difference between the trans and the gauche conformations of −0.35 kcal/mol is obtained. This difference is similar to that of the POL(q_w, μ) model, yielding similar conformational proportions (Table 3). However, the polarization free energy contribution for the two conformations is now smaller (Table 2). This reduction is the result of neglecting the polarization energy associated with the 1−2 and 1−3 bonded interactions.

For the simplest polarization model, POL(q_w), the polarization free energy values, $\Delta G^{\mathrm{POL}}(q_w)$, obtained for each conformation are shown in Table 2. Each free energy value corresponds to an average of four FEP simulations. It can be seen that the gauche conformation is more stabilized than the trans conformation as in the previous models. As the global free energies of polarization of the trans and gauche conformations are similar to that of the POL(q_w, $\mu_{1,4}$) model, the polarization energy associated with the intramolecular interactions between induced dipole moments separated by more than three bonds can be considered small.

To sum up, the total free energies obtained for the three polarization models are −0.28 kcal/mol [POL(q_w, μ)], −0.35 kcal/mol [POL(q_w, $\mu_{1,4}$)], and −0.31 kcal/mol [POL(q_w)]. With these free energies, the calculated gauche proportions are 76% [POL(q_w, μ)], 78% [POL(q_w, $\mu_{1,4}$)], and 77% [POL(q_w)]. Thus, the three polarization models yield similar results. The more populated conformation is the gauche minimum, although its value is slightly greater than that corresponding to the experimental gauche proportion (67%).

To analyze the importance of the polarization contribution, the total free energy of the conformational equilibrium calculated at the LJ + Q level (0.2 ± 0.1 kcal/mol) and the LJ + Q + POL(q_w) level (−0.3 ± 0.1 kcal/mol) can be compared with the experimental value (−0.02 ± 0.03 kcal/mol). Taking into account the statistical errors of the contributions, it can be concluded that the polarization forces introduce a significant free energy change of about −0.5 kcal/mol. The comparison of the total free energy of the polarization model with the experimental value indicates that the gauche conformation is overstabilized. In part, this deviation could come from using solute LJ parameters derived from nonpolarizable molecules that implicitly contain some polarization effects. On the other hand, new sets of atomic polarizability values reparametrized for this

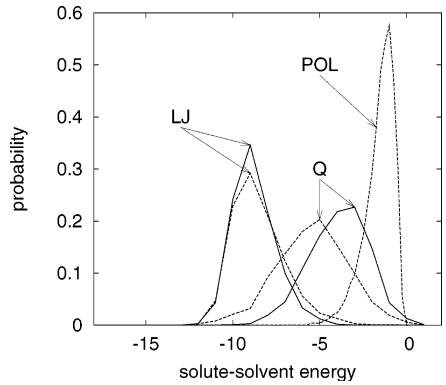

Figure 2. LJ and electrostatic (Q) solute−solvent energy distribution for the trans conformation obtained with the nonpolarizable LJ + Q model (solid line) and the polarizable POL(q_w) potential model (dashed line). The polarization energy distribution (POL) for the POL(q_w) model is also shown. Energy is in kcal/mol.

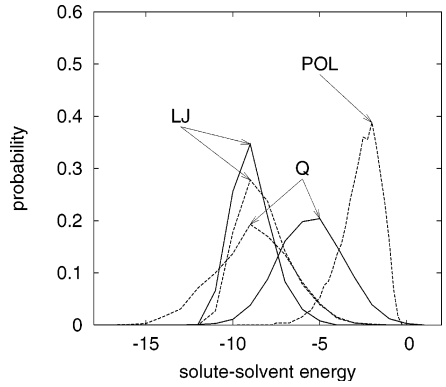

Figure 3. LJ and electrostatic (Q) solute−solvent energy distribution for the gauche conformation obtained with the nonpolarizable LJ + Q model (solid line) and the polarizable POL(q_w) potential model (dashed line). The polarization energy distribution (POL) for the POL(q_w) model is also shown. Energy is in kcal/mol.

type of simulations (polarizable solute and nonpolarizable solvent molecules) could yield more accurate results than those derived from the Applequist model.

3.4. Energetic and Structural Results. The solvation differences between the trans and gauche DCE conformers have been analyzed. The distribution of the solute−solvent LJ, electrostatic, and polarization energy terms have been computed for each conformation using the simulations with the POL(q_w) polarization model and those without the polarization potential model (LJ + Q). For the trans conformation (Figure 2), it can be observed that the distributions of the LJ and electrostatic energy terms suffer significant variations when the polarization is introduced. In particular, the probability of the maximum of the solute−solvent LJ energy distribution is decreased when the polarization model is used, whereas the solute−solvent electrostatic energy distribution is shifted to more stable energies. In Figure 3, a similar behavior for the gauche conformation can be observed. However, the shift of the electrostatic contribution is now greater. These shifts can be quantified with the mean value of each energy term distribution. So, for the trans conformation, the LJ solute−solvent energy is destabilized at about 0.3 kcal/mol and the mean value of the electrostatic solute−solvent energy is stabilized at about 1.5 kcal/mol (Tables 4 and 5). On the other hand, the stabilization of the electrostatic mean energy value of the gauche conformation is greater (3.3 kcal/mol), and at the same time, the mean value of the polarization energies is shifted to a lower value. It can be interpreted that the presence of the polarization forces in the force field reduces the average solute−solvent distances, destabilizing the LJ energy terms but stabilizing the electrostatic contributions.

TABLE 4: LJ and Electrostatic Components of the Total Solute−Solvent Interaction Energy Obtained with the MC Simulations Performed with a Potential Model Including LJ and Electrostatic Contributions (LJ + Q)[a]

conformation	U_{SX}^{LJ}	U_{SX}^{qq}
trans	−8.76 (0.02)	−3.92 (0.04)
gauche	−8.87 (0.02)	−5.51 (0.04)

[a] stdev is in parentheses. Energies are in kcal/mol.

TABLE 5: LJ, Electrostatic, and Polarization Components of the Total Solute−Solvent Interaction Energy Obtained with the MC Simulations with the POL(q_w) Polarization Model[a]

conformation	U_{SX}^{LJ}	U_{SX}^{qq}	U^{POL}
trans	−8.50 (0.03)	−5.44 (0.05)	−1.46 (0.03)
gauche	−8.21 (0.03)	−8.84 (0.05)	−2.54 (0.03)

[a] stdev is in parentheses. Energies are in kcal/mol.

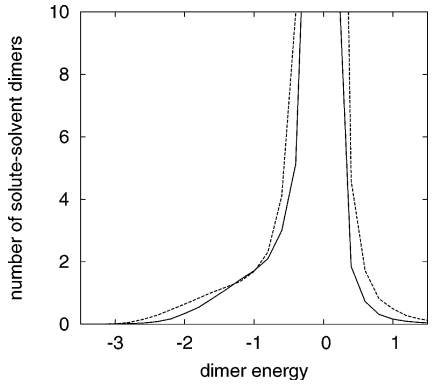

Figure 4. Solute−solvent pairwise (LJ plus electrostatic contributions) dimer energy distributions corresponding to the MC simulations performed with the POL(q_w) potential model for trans (solid line) and gauche (dashed line) DCE conformations in water. Energy is in kcal/mol.

The differential behavior of the pairwise solute−solvent interactions for each DCE conformation was also analyzed using the solute−solvent dimerization distributions (Figure 4). It can be observed that there is a shoulder between an energy of about −3.0 to an energy of about −1.0 kcal/mol that corresponds to the dimerization energies between nearest neighbors and a sharp high peak, near 0 kcal/mol, due to interactions between the many dimers with a large intermolecular distance. The integration of the number of dimers that corresponds to the shoulder yields 6.3 and 7.7 water coordinate molecules for trans and gauche conformations, respectively. Thus, these numbers indicate that there is a greater number of water molecules (1.4) in the first coordination shell of the gauche conformation. Because the sharp peak around 0 kcal/mol is wider for gauche conformation, it indicates that the interaction of a distant molecule with the solute ranges in a wider interval for this conformation. This is a consequence of the difference in the molecular dipole moment between both solute conformations.

Differences in the structural disposition of solvent molecules around each solute conformation can be seen with the solute−solvent radial distribution function defined between the central point of the C−C bond in the DCE and the O atom of the water molecule (Figure 5). The first peak of the gauche radial distribution presents a shoulder around 3.0 Å that is not present in the trans distribution. The integration until 3.5 Å yields a

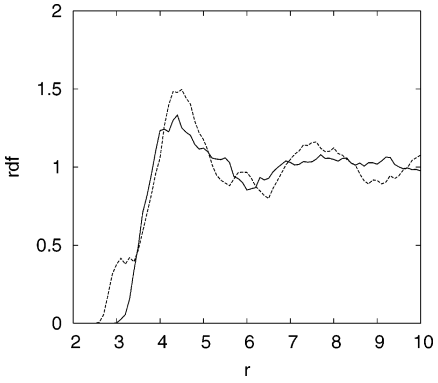

Figure 5. Solute−solvent radial distribution functions for the center of the solute C−C bond and the oxygen water atom obtained for the trans (solid line) and gauche (dashed line) DCE conformations. Distance is in Å.

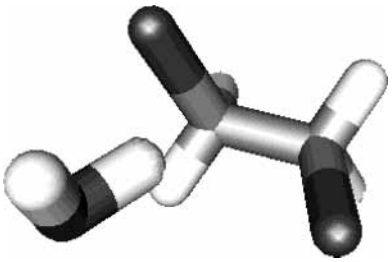

Figure 6. Representation of the DCE molecule with the nearest water molecule to the center of the solute C−C bond taken from a configuration of the POL(q_w) simulations.

value of 1.3 water molecules. The analysis of the solute−solvent interaction energy of these molecules indicates that they also contribute to the shoulder of the dimerization energy distribution of the gauche conformation (Figure 4). From the simulations, different snapshots have been taken to visualize the position of the water molecule nearest to the center of the solute. They show that this molecule is always situated in a small region of the space with a particular orientation with respect to the solute. As it can be seen from one of the snapshots (Figure 6), this water molecule is located in the side of the solute where the Cl atoms are oriented and closer to one of them. One of the H atoms of this water molecule is pointing between the solute Cl atoms, whereas the other H atom is directed toward the bulk. Because the position of this molecule is not in the C_2 symmetry axis of the gauche conformer, there is another symmetrical region to be occupied by another molecule. However, the simultaneous occupation of these two symmetrical regions has not been found in the liquid simulations because this would lead to an important electrostatic repulsion between the H of the two water molecules. On the other hand, in the symmetrical region a water molecule about 0.5 Å more distant from the solute, with an H directed toward its nearest Cl solute atom and the other toward the bulk, has been observed.

The effect of polarization forces over the energetic and structural properties of the solution has been studied by monitoring the electric fields induced by the solvent charges over each solute atom. In Figure 7 the modules of these electric fields (E^q) for the trans and gauche DCE conformations in the polarizable and nonpolarizable simulations are compared. It can be seen that the inclusion of polarization forces increases the E^q values in each solute atom in both the trans and the gauche conformations. This electric field is greater for the gauche conformer because it can be expected from its greater polarization energy obtained in solution. Because the solute Cl atoms show the greatest electric field increase, it can be stated that

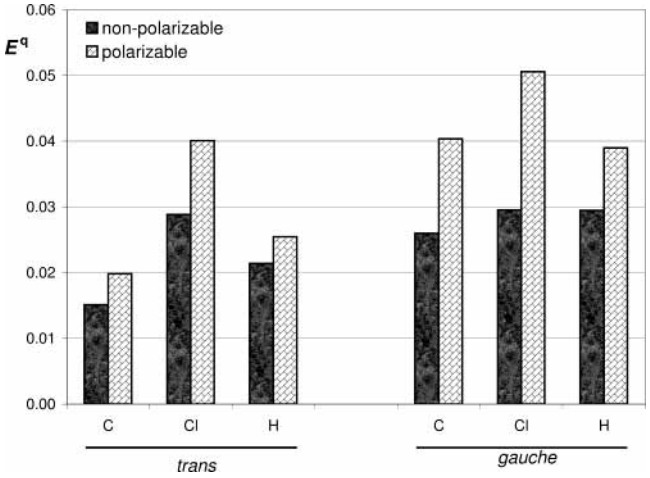

Figure 7. Module of the electric field generated by the solvent charges at each solute atom type for the trans and gauche DCE conformations obtained from the simulations with the nonpolarizable LJ + Q model and the polarizable POL(q_w) potential model. Electric field units are in $(1/4\pi\epsilon_0)(e^-/Å^2)$.

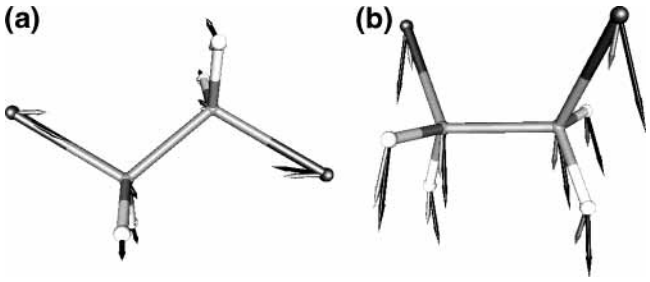

Figure 8. Graphical representation of the electric field generated by the solvent charges at each solute atom for (a) trans and (b) gauche DCE conformations obtained from the simulations with the nonpolarizable LJ + Q model (light arrows) and the polarizable POL(q_w) potential model (dark arrows). The lengths of the arrows of both figures refer to the same arbitrary scale.

the reorganization of the solvent molecules is greater around them. That is probably a consequence of factors such as its highest polarizabily value and its bigger contact surface with the solvent. The orientations of these electric fields for polarizable and nonpolarizable simulations have also been analyzed for both conformations (Figure 8). In the trans conformation, the $\vec{E}^q$ vectors present opposite orientations between pairs of the same atom types. Particularly, the electric fields generated over the solute Cl atoms are oriented toward the center of the molecule. This orientation is caused by the preferential orientation of the H atoms of the surrounding water molecules that are attracted by the negative charge value of the Cl atoms. On the contrary, the electric fields generated over the solute H atoms are oriented toward the bulk as a consequence of their positive charge. On the other hand, in the gauche conformation, it can be seen that the $\vec{E}^q$ vectors on all solute atoms are similarly oriented. The dipole moment induced in the solute molecule can be interpreted in terms of the orientation of all $\vec{E}^q$ vectors. Particularly, in the POL(q_w) model this interpretation can be done directly because the orientation of the dipole moment induced on a solute atom coincides with the orientation of the $\vec{E}^q$ vector defined on this atom (eq 14). Thus, in the trans conformation (Figure 8a), the orientation of the induced dipole moments of each atom makes practically null the net induced dipole moment of the solute. On the other hand, in the gauche conformation (Figure 8b), the collective effect of the induced dipole moments of all atoms reinforces the permanent dipole

moment of the solute. Finally, it can be seen in Figure 8 that the observed differences in the orientation of the $\vec{E}^q$ vectors between the nonpolarizable model (light arrows) and the polarizable model (dark arrows) for both the trans and the gauche conformations are another evidence that the introduction of the polarization forces in the force field of the system leads to a reorganization of the solvent molecules.

4. Conclusions

The conformational equilibrium of DCE in water has been studied with FEP simulations. The calculation of the relative solvation free energy of trans and gauche solute conformations has been decomposed in LJ transformations between structures, discharge, and polarization processes. This strategy allows evaluation of the importance of each energetic term in the position of the conformational equilibrium.

With an only LJ description of the solute molecule, the obtained conformational equilibrium in water is similar to the conformational equilibrium in the gas phase. As the experimental data indicate a large influence of the solvent in the stabilization of the gauche conformer, the conformational change of DCE induced by solvation is not reproduced with this model. The dipole moment of solute conformations cannot be neglected.

When the solvation free energy contribution due to the inclusion of electrostatic solute−solvent interactions is calculated for each conformation, the obtained global free energy difference is reduced and the conformational equilibrium is moved to the gauche conformation (58%). Thus, the inclusion of the electrostatic contribution favors the stabilization of the solute conformation with a nonzero dipole moment, obtaining conformational populations near the experimental value (67%).

The role of polarization forces is analyzed by means of three polarization models that differ in the way the intramolecular interactions among the polarizations sites of DCE are treated. Despite their differences, the three polarization models yield similar conformational results. Thus, the conformational equilibrium of DCE in water can be studied with the most simple polarization model which considers no interaction between induced dipole moments of the solute atoms. The most populated conformation is the gauche minimum (77%), although the obtained proportion is slightly greater than that corresponding to the experimental value. The calculations show that the polarization forces introduce a significant free energy change of about −0.5 kcal/mol. However, both conformational results, from the polarizable and nonpolarizable models, are relatively near the experimental proportions of DCE in water. It has been seen that these experimental proportions could be reproduced with a polarization energy contribution of only −0.2 kcal/mol. Thus, the polarization energy is overestimated for the three polarization models, indicating the need of a better parametrization of the atomic interaction parameters.

The overall results show that the improvement in the solute conformational proportions can be obtained considering only the polarization of the solute molecule and maintaining a nonpolarizable solvent model. This approach yields reasonable results without a marked increase of computational costs.

The presence of the polarization forces in the force field reduces the average solute−solvent distances, destabilizing the LJ energy terms but stabilizing the electrostatic contributions. Thus, for the trans and gauche conformations the distributions of the LJ and electrostatic energy terms suffer significant variations when the polarization is introduced. These shifts are greater for the gauche conformation.

Differences in the structural disposition of solvent molecules around each solute conformation can be seen with the solute−solvent radial distribution functions and with the analysis of the electrostatic fields. It has been observed that the orientation of the induced dipole moments of each atom makes practically null the net induced dipole moment of the trans conformation of the solute, whereas in the gauche conformation, the collective effect of the induced dipole moments of all atoms reinforces the permanent dipole moment of the DCE molecule.

Acknowledgment. Financial support from the Spanish Ministerio de Ciencia y Tecnología (Project No. BQU2003-09698-CO2-02) and from the Comissionat per a Universitats i Recerca de la Generalitat de Catalunya (2001SGR00301) is acknowledged. The Centre de Supercomputació de Catalunya C^4-CESCA is also acknowledged for providing us with computer capabilities. S. M. benefited from a grant of Universitat de Barcelona.

References and Notes

(1) Wiberg, K. B.; Keith, T. A.; Frisch, M. J.; Murcko, M. *J. Phys. Chem.* **1995**, *99*, 9072.
(2) Wong, M. W.; Frisch, M. J.; Wiberg, K. B. *J. Am. Chem. Soc.* **1991**, *113*, 4776.
(3) Stolov, A. A.; Remizov, A. B. *Spectrochim. Acta, Part A* **1995**, *51*, 1919.
(4) Jorgensen, W. L.; McDonald, N. A.; Selmi, M.; Rablen, P. R. *J. Am. Chem. Soc.* **1995**, *117*, 11809.
(5) Kaminski, G. A.; Jorgensen, W. L. *J. Phys. Chem. B* **1998**, *102*, 1787.
(6) Bigot, B.; Costa-Cabral, B. J.; Rivail, J. L. *J. Chem. Phys.* **1985**, *83*, 3083.
(7) Benjamin, I.; Pohorille, A. *J. Chem. Phys.* **1993**, *98*, 236.
(8) Beutler, T. C.; Gunsteren, W. F. *J. Chem. Phys.* **1994**, *100*, 1492.
(9) Soriano, A.; Silla, E.; Tuñón, I. *J. Phys. Chem. B* **2003**, *107*, 6234.
(10) Depaepe, J.-M.; Ryckaert, J.-P. *Chem. Phys. Lett.* **1995**, *245*, 653.
(11) Millot, C.; Rivail, J. L. *J. Mol. Liq.* **1989**, *43*, 111.
(12) Millot, C.; Rivail, J. L. *Mol. Phys.* **1992**, *77*, 157.
(13) Jorgensen, W. L.; Binning, R. C., Jr.; Bigot, B. *J. Am. Chem. Soc.* **1981**, *103*, 4393.
(14) Scarsi, M.; Apostolakis, J.; Caflisch, A. *J. Phys. Chem. B* **1998**, *102*, 3637.
(15) Vilaseca, E. *J. Chem. Phys.* **1996**, *104*, 4243; **1999**, *110*, 5473.
(16) Hernández, B.; Curutchet, C.; Colominas, C.; Orozco, M.; Luque, F. J. *Mol. Sim.* **2002**, *28*, 153.
(17) Caldwell, J. W.; Kollman, P. A. *J. Am. Chem. Soc.* **1995**, *117*, 4177.
(18) Eriksson, M. A. L.; Morgantini, P. Y.; Kollman, P. A. *J. Phys. Chem. B* **1999**, *103*, 4474.
(19) Caldwell, J. W.; Kollman, P. A. *J. Am. Chem. Soc.* **1995**, *92*, 6761.
(20) Meng, E. C.; Caldwell, J. W.; Kollman, P. A. *J. Phys. Chem.* **1996**, *100*, 2367.
(21) Chang, T. M.; Dang, L. X. *J. Chem. Phys.* **1996**, *104*, 6772.
(22) Dang, L. X. *J. Chem. Phys.* **1999**, *110*, 10113.
(23) Sun, Y.; Caldwell, J. W.; Kollman, P. A. *J. Phys. Chem.* **1995**, *99*, 1008.
(24) Koneshan, S.; Rasaiah, J. C.; Dang, L. X. *J. Chem. Phys.* **2001**, *114*, 7544.
(25) Madurga, S.; Vilaseca, E. *J. Phys. Chem. A* **2002**, *106*, 11822.
(26) Jedlovszky, P.; Richardi, J. *J. Chem. Phys.* **1999**, *110*, 8019.
(27) Yoshii, N.; Yoshie, H.; Miura, S.; Okazaki, S. *J. Chem. Phys.* **1998**, *109*, 4873.
(28) Jedlovszky, P.; Mezei, M.; Vallauri, R. *Chem. Phys. Lett.* **2000**, *318*, 155.
(29) Caldwell, J. W.; Kollman, P. A. *J. Phys. Chem.* **1995**, *99*, 6208.
(30) Cubero, E.; Luque, F. J.; Orozco, M. *Proc. Natl. Acad. Sci. U.S.A.* **1998**, *95*, 5976.
(31) Mo, Y.; Subramanian, G.; Gao, J.; Ferguson, D. M. *J. Am. Chem. Soc.* **2002**, *124*, 4832.
(32) Chen, B.; Xing, J.; Siepmann, J. I. *J. Phys. Chem. B* **2000**, *104*, 2391.
(33) Liu, Y.-P.; Kim, K.; Berne, B. J.; Friesner, R. A.; Rick, S. W. *J. Chem. Phys.* **1998**, *108*, 4739.
(34) González, M. A.; Enciso, E.; Bermejo, F. J., Bée, M. *J. Chem. Phys.* **1999**, *110*, 8045.
(35) Dang, L. X. *J. Chem. Phys.* **2000**, *113*, 266.
(36) Jedlovszky, P.; Vallauri, R. *J. Chem. Phys.* **2001**, *115*, 3750.
(37) Stern, H. A.; Rittner, F.; Berne, B. J.; Friesner, R. A. *J. Chem. Phys.* **2001**, *115*, 2237.
(38) Ribeiro, M. C. C. *Phys. Rev. B* **2001**, *63*, 94205.
(39) Soetens, J. C.; Jansen, G.; Millot, C. *Mol. Phys.* **1999**, *96*, 1003.

(40) Kaminski, G. A.; Stern, H. A.; Berne, B. J.; Friesner, R. A. *J. Phys. Chem. A* **2004**, *108*, 621.
(41) Cieplak, P.; Caldwell, J. W.; Kollman, P. A. *J. Comput. Chem.* **2001**, *22*, 1048.
(42) Halgren, T. A.; Damm, W. *Curr. Opin. Struct. Biol.* **2001**, *11*, 236.
(43) Applequist, J. *Acc. Chem. Res.* **1977**, *10*, 79.
(44) Gresh, N.; Sponer, J. *J. Phys. Chem. B* **1999**, *103*, 11415.
(45) Banks, J. L.; Kaminski, G. A.; Zhou, R.; Mainz, D. T.; Berne, B. J.; Friesner, R. A. *J. Chem. Phys.* **1999**, *110*, 741.
(46) Stern, H. A.; Kaminski, G. A.; Banks, J. L.; Zhou, R.; Berne, B. J.; Friesner, R. A. *J. Phys. Chem. B* **1999**, *103,* 4730.
(47) Dehez, F.; Soetens, J. C.; Chipot, C.; Ángyán, J. G.; Millot, C. *J. Phys. Chem. A* **2000**, *104*, 1293.
(48) Dehez, F.; Chipot, C.; Millot, C.; Ángyán, J. G. *Chem. Phys. Lett.* **2001**, *338*, 180.
(49) Chipot, C.; Dehez, F.; Ángyán, J. G.; Millot, C.; Orozco, M.; Luque, F. J. *J. Phys. Chem. A* **2001**, *105*, 11505.
(50) Madurga, S.; Paniagua, J. C.; Vilaseca, E. *Chem. Phys.* **2000**, *255*, 123.
(51) Owicki, J. C.; Scheraga, H. A. *Chem. Phys. Lett.* **1977**, *47*, 600.
(52) Owicki, J. C. *ACS Symp. Ser.* **1978**, *86*, 159.
(53) Allen, M. P.; Tildesley, D. J. *Computer Simulation of Liquids*; Oxford University Press: Oxford, 1987.
(54) Schmidt, M. W.; Baldridge, K. K.; Boatz, J. A.; Elbert, S. T.; Gordon, M. S.; Jensen, J. J.; Koseki, S.; Matsunaga, N.; Nguyen, K. A.; Su, S.; Windus, T. L.; Dupuis, M.; Montgomery, J. A. *J. Comput. Chem.* **1993**, *14*, 1347.
(55) Jorgensen, W. L.; Madura, J. D. *Mol. Phys.* **1985**, *56*, 1381.
(56) Applequist, J.; Carl, J. R.; Fung, K.-K. *J. Am. Chem. Soc.* **1972**, *94*, 2952.
(57) Cappelli, C.; Corni, S.; Tomasi, J. *J. Phys. Chem. A* **2001**, *105*, 10807.
(58) Kato, M.; Abe, I.; Taniguchi, Y. *J. Chem. Phys.* **1999**, *110*, 11982.